Journal of Biomechanics 82 (2019) 211–219

Contents lists available at ScienceDirect

Journal of Biomechanics

journal homepage: www.elsevier.com/locate/jbiomech
www.JBiomech.com

Contributions of Glycosaminoglycans to Collagen Fiber Recruitment in Constitutive Modeling of Arterial Mechanics

Jeffrey M. Mattson [a], Yunjie Wang [a], Yanhang Zhang [a,b,*]

[a] Department of Mechanical Engineering, Boston University, Boston, MA 02215, USA
[b] Department of Biomedical Engineering, Boston University, Boston, MA 02215, USA

ARTICLE INFO

Article history:
Accepted 23 October 2018

Keywords:
Fiber recruitment
Structure-based constitutive model
Glycosaminoglycans
Collagen
Elastin

ABSTRACT

The contribution of glycosaminoglycans (GAGs) to the biological and mechanical functions of biological tissue has emerged as an important area of research. GAGs provide structural basis for the organization and assembly of extracellular matrix (ECM). The mechanics of tissue with low GAG content can be indirectly affected by the interaction of GAGs with collagen fibers, which have long been known to be one of the primary contributors to soft tissue mechanics. Our earlier study showed that enzymatic GAG depletion results in straighter collagen fibers that are recruited at lower levels of stretch, and a corresponding shift in earlier arterial stiffening (Mattson et al., 2016). In this study, the effect of GAGs on collagen fiber recruitment was studied through a structure-based constitutive model. The model incorporates structural information, such as fiber orientation distribution, content, and recruitment of medial elastin, medial collagen, and adventitial collagen fibers. The model was first used to study planar biaxial tensile stress-stretch behavior of porcine descending thoracic aorta. Changes in elastin and collagen fiber orientation distribution, and collagen fiber recruitment were then incorporated into the model in order to predict the stress-stretch behavior of GAG depleted tissue. Our study shows that incorporating early collagen fiber recruitment into the model predicts the stress-stretch response of GAG depleted tissue reasonably well (rms = 0.141); considering further changes of fiber orientation distribution does not improve the predicting capability (rms = 0.149). Our study suggests an important role of GAGs in arterial mechanics that should be considered in developing constitutive models.

1. Introduction

Pathogenesis of many vascular diseases, including hypertension, atherosclerosis, stenosis, and aneurysms has been associated with ECM disorders in structure and function and its altered interaction with other arterial constituents. Studies of the structural components of arteries are generally focused on elastin and collagen (Boumaza et al., 2001; Brüel and Oxlund, 1996; Campa et al., 1987; Humphrey and Holzapfel, 2012; Martinez-Lemus et al., 2009; Menashi et al., 1987; Vorp, 2007). Once thought of as simply components of connective tissue, over the last decade the functional and regulatory significance of proteoglycans (PGs) has emerged as a promising field in all aspects of cell biology and human diseases (Halper, 2014). Recent research suggested an important role of GAGs in binding of low-density lipoprotein, or bad cholesterol, to the arterial wall (Little et al., 2007). When proteoglycans are in excess, they play a major role in the formation of atherosclerotic lesions due to the retention of low-density lipoprotein (Huang et al., 2008; Wight and Merrilees, 2004). Localized accumulation/pooling of proteoglycans can cause arterial wall layers to dissect from increased Donnan swelling pressure (Humphrey, 2012; Sorrentino et al., 2015). In contrast, insufficient levels of the proteoglycans reduce the arteries ability to regulate charge/structure and could play a role in diabetes (Jensen, 1997). Proteoglycans deficiency was also suggested to lead to aortic rupture by comprising the functionality of other structural components (Heegaard et al., 2007).

The basic PG unit consists of a "core protein" with one or more covalently attached glycosaminoglycan (GAGs) chains. PGs are found in all connective tissues. They provide structural basis for multiple biological functions, such as the organization of ECM assembly and the regulation of cell growth factors. PGs provide appropriate spacing and organization for other ECM components (Gandley et al., 1997). Since GAGs have a high affinity for water molecules, they serve to hydrate the ECM but also can resist deformation (Lee et al., 2001). The highly charged aggregates also interact with other ECM components, for example, decorin is a PG

* Corresponding author at: 110 Cummington Mall, Boston, MA 02215, USA.
E-mail address: yanhang@bu.edu (Y. Zhang).

https://doi.org/10.1016/j.jbiomech.2018.10.031
0021-9290/

known to bind to type I collagen (Halper, 2014). Electron microscopy and immunofluorescence studies strongly suggest the association of PGs with specific regions of the banding pattern of collagen fibrils and also indicate that PGs can form bridges between fibrils (Bartholomew and Anderson, 1983; Eisenstein and Kuettner, 1976; Lewis et al., 2010; Scott, 2003). Furthermore, PGs appear to bind to many cell-surface receptors with high specificity, thereby activating signaling pathways that control cell proliferation, differentiation, adhesion, and migration (Schaefer and Schaefer, 2010).

Various models have been developed to consider GAGs in connective tissue mechanics. Biphasic and triphasic theories have been developed to model cartilage mechanics, first based on the solid collagen-GAG phase and viscous fluid phase, then followed by the addition of a third ionic phase (Lai et al., 1991; Mow et al., 1980). In tendon mechanics, GAGs are modeled as cross-linking collagen to transfer stretch or isolating neighboring collagen fibrils to promote sliding (Rigozzi et al., 2013; Scott, 2003). In lung tissue mechanics, GAGs have been modeled as contributing to a spring network model that maintains stability of alveolar structure (Takahashi et al., 2014). In carotid artery mechanics, a constitutive model demonstrated that GAGs can cause local intramural swelling that affects structural integrity and mechanosensing (Sorrentino et al., 2015). Recently, a multiscale model was developed to incorporate GAGs protecting collagen fibrils from over-stretching (Linka et al., 2016). In a structurally-based constitutive model of porcine aorta, GAGs were considered to transfer load among collagen fibers through the stiffness of collagen-GAG complexes (Polzer et al., 2015). In a recent study, we found that GAG depletion resulted in earlier nonlinear stiffening of porcine aorta, as well as straighter collagen fibers being recruited at lower strain (Mattson et al., 2016). These findings suggest that GAGs play an important role in arterial mechanics indirectly by affecting the engagement of collagen fibers. In this study, collagen engagement was studied based on multiphoton imaging analysis for intact aorta and GAG depleted porcine aorta. The engagement function of medial and adventitial collagen was then determined, and incorporated into a structure-based constitutive model (Wang et al., 2016).

2. Materials and methods

2.1. Determination of fiber recruitment function

Representative images of intact aorta show adventitial collagen, medial collagen, and medial elastin (Fig. 1). The bundles of wavy adventitial collagen fibers straighten with stretch (Fig. 1a,b). The medial collagen shows a more intricate network with tighter crimp (Fig. 1c). The medial elastin fiber network is visibly distinguished by lacking the characteristic crimp of collagen (Fig. 1d). Straightness parameter and fractal analysis provided insightful information on changes in fiber network structure in response to mechanical loading (Mattson et al., 2016). Straightness parameter provides direct information about the traced straightening and recruitment of adventitial collagen fibers at different strain levels. Therefore, the distribution of straightness parameter measurements was obtained to provide the proportion of fibers recruited at each strain level. Specifically, a recruitment threshold of 0.98 was set and cumulative fiber recruitment was determined.

Since straightness parameter tracing cannot be done for the intricate medial collagen fibers, fractal analysis serves as a broad measure of fiber recruitment for both adventitial and medial collagen. Details about the fractal analysis method can be found from Li et al. (2009) and our earlier work (Chow et al., 2014). Briefly, fractal analysis was performed through a box-counting protocol in ImageJ (https://imagej.nih.gov/ij/), which gives a fractal dimension that represents the self-similarity of an image. The fractal number shows a trend of changing due to straightening of fibers during recruitment, but minimal changes during delayed fiber recruitment as well as after fibers are fully recruited and straightened (Chow et al., 2014; Mattson et al., 2016). Thus, fiber recruitment was assumed to occur over the increments of stretch in which fractal analysis shows an increasing trendline. Therefore, fiber recruitment functions of adventitial collagen (AC) and medial collagen (MC) were fit to the fractal analysis results of images before and after enzymatic GAG depletion at 0–40% stretch, using the fiber recruitment function (Lanir, 1979):

$$\eta_f^i = \frac{1}{\sqrt{2\pi}d_i} exp\left[-\frac{(x-m_i)^2}{2d_i^2}\right] \tag{1}$$

where x is the stretch, and m_i and d_i (i = AC and MC) are the mean and standard deviation of the fiber recruitment function, which were chosen to fit the stretch ranges where the fractal analysis shows an increasing trendline.

2.2. Constitutive modeling

In order to consider the contribution of GAGs to fiber recruitment, a structure-based constitutive model that was previous developed by Wang et al. (2016) was adapted in this study. Briefly, the model allows direct incorporation of information obtained from quantitative multiphoton imaging analysis and biochemical assays for the prediction of tissue-level mechanical properties. The model considers the contribution from medial elastin (ME), medial collagen (MC), and adventitial collagen (AC), incorporating relative collagen and elastin contents, n_i, fiber orientation distributions, $R_i(\theta)$, and fiber recruitment (i = *ME*, *MC*, and *AC*).

In this study, considering the close association between GAGs and collagen fiber assembly, fiber recruitment function determined from fractal analysis, η_f^{MC} and η_f^{AC}, are included for medial and adventitial collagen, respectively. The total strain energy function of the arterial wall is the sum of the constituent strain energy, and can be written as:

$$W = n_{ME}\int_{-\pi/2}^{\pi/2}\psi_{ME}R_{ME}(\theta)d\theta + n_{MC}\int_{-\pi/2}^{\pi/2}\int_{1}^{\lambda}\psi_{MC}(\lambda-x)\eta_f^{MC}dxR_{MC}(\theta)d\theta + n_{AC}\int_{-\pi/2}^{\pi/2}\int_{1}^{\lambda}\psi_{AC}(\lambda-x)\eta_f^{AC}dxR_{AC}(\theta)d\theta \tag{2}$$

where n_i is the content for each component, R_i is the fiber orientation distribution function, which was obtained from our previous studies with two-dimensional fast Fourier transform analysis (Chow et al., 2014; Mattson et al., 2016; Wang et al., 2016). In this study, the fiber orientation distributions at 40% equibiaxial strain was used to reveal the fiber orientation distributions when the fibers are straightened (Fig. 2). ψ_i (i = *ME*, *MC*, and *AC*) is the fiber level strain energy function, which is defined by a freely-jointed chain model as (Wang et al., 2016):

$$\psi_i = k\Theta N_i\left(\frac{\rho_i}{N_i}\beta_\rho^i + \ln\frac{\beta_\rho^i}{\sinh\beta_\rho^i}\right) - k\Theta\beta_p^i\ln\lambda_f \tag{3}$$

where $k = 1.38\times10^{-23}$ J/K is Boltzmann's constant, Θ = 298 K is the absolute temperature, N_i is the number of rigid links within each chain, ρ_i is the normalized deformed chain length, P_i is the normalized undeformed length, λ_f is the fiber-level stretch and $\beta_\rho^i = L^{-1}(\frac{\rho_i}{N_i})$, where $L(x) = \coth x - 1/x$ is the Langevin function. The tissue-level Cauchy stress can be obtained from $\sigma = J^{-1}FSF^T$, where $S = \frac{\partial W}{\partial E}$ is the second Piola-Kirchhoff stress, and F is the deformation gradient, and J = det(F).

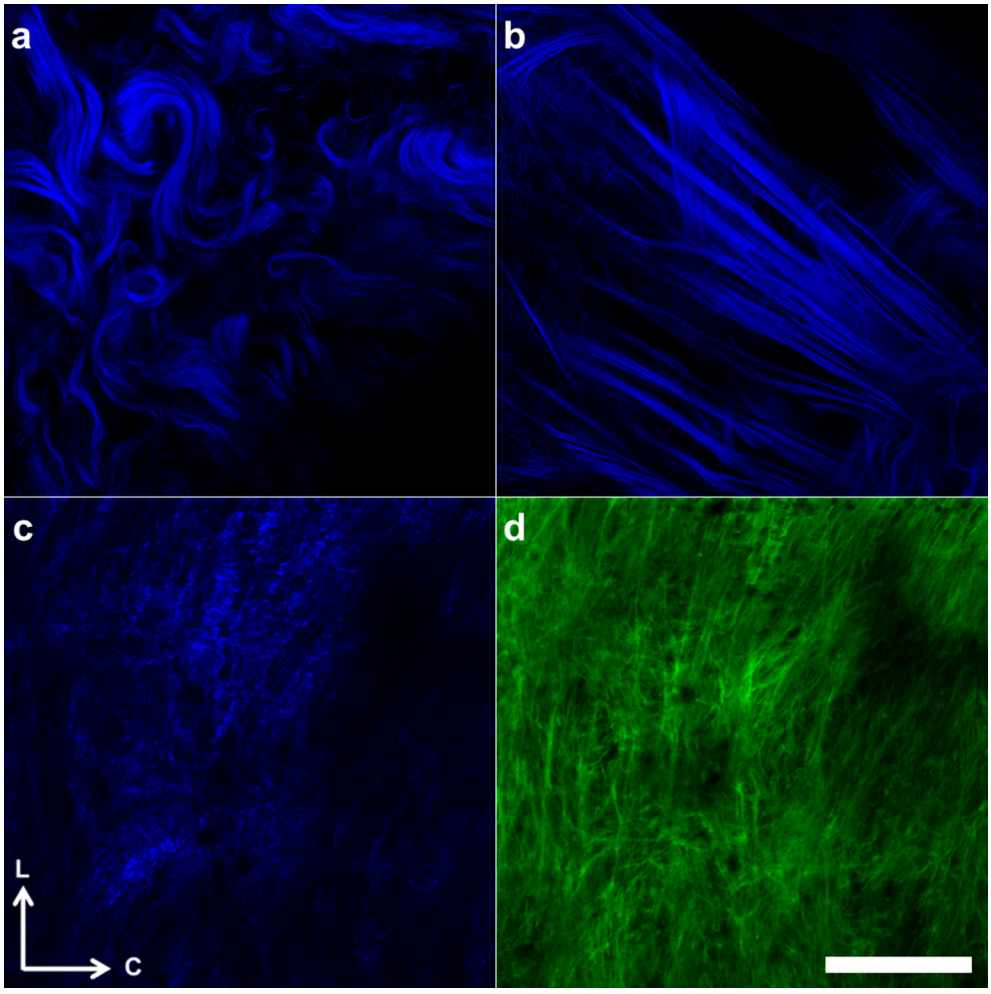

Fig. 1. Multiphoton images of intact porcine thoracic aorta showing that adventitial collagen fibers are wavy (a), but straighten with stretch (b). Fiber recruitment for the finer medial collagen (c) and medial elastin (d) fiber networks are detectable with fractal analysis. Horizontal is circumferential (C) and vertical is longitudinal (L). Images are 360 μm × 360 μm, scale bar is 100 μm.

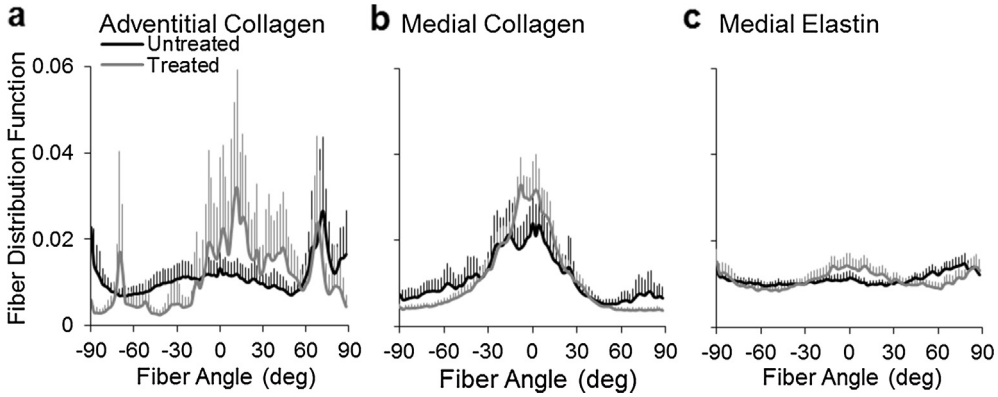

Fig. 2. Average fiber distributions (n = 6) at 40% stretch for untreated (black) and treated (gray) tissue with circumferentially and longitudinally oriented fibers corresponding to 0° and ±90°, respectively. After treatment, adventitial collagen (a) becomes more circumferentially orientated, whereas medial collagen (b) remains circumferentially oriented and medial elastin (c) remains relatively uniformly distributed. Untreated data from (Chow et al., 2014) and treated data from (Mattson et al., 2016).

2.3. Parameters estimation

The model has six material parameters: N_i and n_i ($i = ME$, MC, and AC). The model was first fit to the average planar equi- and nonequi-biaxial tensile stress-stretch data of porcine thoracic aorta (Mattson et al., 2016). Material parameter n_i ($1/m^3$) is related to the mass content of ECM constituents. They are reinforced to satisfy the constraints $0.4614(n_{MC} + n_{AC}) < n_{ME} < 2.8315(n_{MC} + n_{AC})$ based on our previous biochemical assay measurements of elastin and collagen contents (Chow et al., 2013a, Chow et al., 2013b). $n_i k\Theta$ is related to the initial stiffness of the ECM constituent (Zhang et al., 2005). Material parameter N_i largely determines where the

strain stiffening starts and is assumed to satisfy the relationship of $N_{ME} > N_{MC} > N_{AC} > 1$ so that the stiffness of medial elastin < medial collagen < adventitial collagen. The material parameters were determined by minimizing the objective function with appropriate constraints (Wang et al., 2016):

$$E = \sum_{j=1}^{m} \left[\left(\sigma_{11}^{c} - \sigma_{11}^{e}\right)_j^2 + \left(\sigma_{22}^{c} - \sigma_{22}^{e}\right)_j^2 \right] \quad (4)$$

where m is the number of data points and σ^c and σ^e represent Cauchy stress from the model and biaxial tensile tests, respectively. Subscripts 1 and 2 correspond to the longitudinal and circumferential directions of the aortic sample, respectively. The objective function is minimized using the Nelder–Mead direct search method implemented in the fminsearch subroutine in MATLAB (version R2013b, MathWorks, Inc.). As a measure of goodness of fit, the root mean square error is defined as (Holzapfel et al., 2005):

$$e = \frac{\sqrt{\frac{E}{m-q}}}{\sigma_{ref}} \quad (5)$$

where q is the number of parameters in the model, and σ_{ref} is determined from the sum of experimental Cauchy stresses in both circumferential and longitudinal directions divided by the number of data points *m*.

The obtained model parameters were then used to predict the average biaxial stress-stretch response of GAG depleted tissue (Mattson et al., 2016). Changes in elastin and collagen fiber distribution, and collagen fiber recruitment with GAG depletion were incorporated into the model. To understand the effect of these changes on tissue mechanics, first predictions were made in which only changes in collagen fiber recruitment functions were considered. Then predictions were made when changes in both fiber distributions and fiber recruitment functions were considered.

3. Results

The distributions of straightness parameters at each level of stretch demonstrate that fibers of intact aorta tend to have a lower straightness parameter compared to GAG depleted tissue (Fig. 3). In general, straightness parameter increases with stretch, visualized by the bar graphs shifting and clustering to the right, asymptotically approaching 1, which represents a straight line. However, at each level, fibers in intact aorta tend to be wavier with straightness parameters present to the left of fibers from GAG depleted tissue. To examine the adventitial collagen fiber recruitment, cumulative fiber recruitment was determined where fibers with a straightness parameter of at least 0.98 were considered to be recruited (Fig. 4). Results in Fig. 4 further shows that there are more recruited fibers for GAG depleted versus intact tissue at each level of stretch until almost all fibers are recruited for both conditions at 1.4 stretch.

Since elastin fibers respond to immediate deformation, fiber recruitment functions, η_f^{AC} and η_f^{MC}, were only determined for adventitial and medial collagen (Fig. 5). Increments of stretch where the fractal analysis trendline is increasing indicates fiber recruitment. Therefore, parameters *m* and *d*, the mean and standard deviation of the fiber recruitment function, were chosen based on the stretch range of adventitial and medial collagen that corresponded with an increasing fractal analysis trendline. With GAG depletion, the recruitment function shifts to a lower and smaller stretch range. For adventitial collagen, η_f^{AC} spanned ~1.15

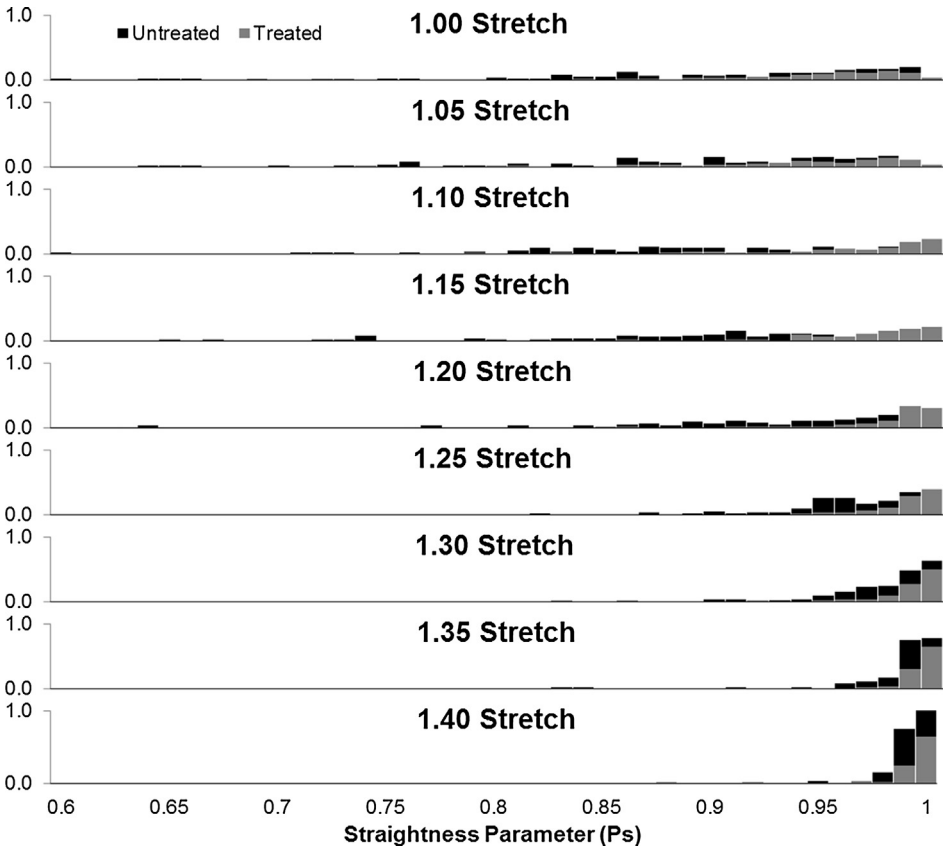

Fig. 3. Straightness parameter distributions of adventitial collagen for each level of stretch for untreated (black) and treated (gray) tissue from Mattson et al. (2016). The number of fibers in each bin were normalized to the total number of fibers traced for each level of stretch for each tissue type.

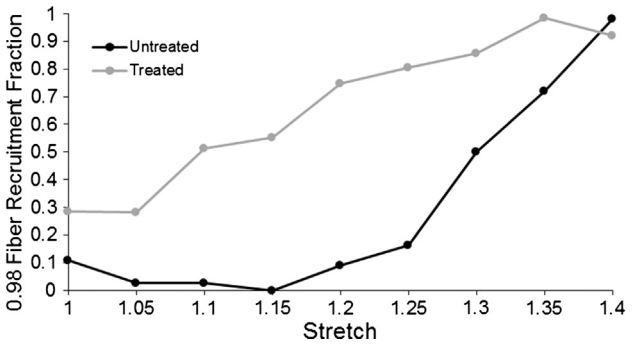

Fig. 4. Cumulative adventitial collagen fiber recruitment for untreated (black) and treated (gray) tissue, where a straightness parameter of at least 0.98 in Fig. 1 qualifies a fiber as recruited.

to ~1.35 stretch for intact tissue (Fig. 5a), but shifted to a lower stretch range of 1 to ~1.15 after GAG removal (Fig. 5b). For medial collagen, η_f^{MC} covered 1–1.4 stretch for intact tissue, but decreased to a stretch range of 1 to ~1.2 after GAG removal (Fig. 5d). The chosen values of m and d were indicated in Fig. 5.

GAG depletion results in straighter collagen fibers that are recruited at lower levels of stretch with a corresponding earlier transition to nonlinear stiffening (Fig. 6). Looking at the stress-stretch curves, the treated tissue stiffens more in the circumferential direction in agreement with the primarily circumferentially oriented GAG depleted adventitial and medial collagen fibers (Figs. 5 and 6). The model was fit to the biaxial stress-stretch data of intact aorta to determine the model parameters (rms = 0.135). The same model parameters were then used to predict the stress-stretch response of GAG depleted tissue considering changes in fiber recruitment (Fig. 6). Overall, the model is able to characterize the nonlinear, anisotropic behavior with a small overestimate in the longitudinal direction at higher stiffness and small underestimate in the circumferential direction. There is a slight overestimate of the nonlinear stiffening in the circumferential direction after GAG depletion. In Fig. 7, prediction results from using the treated fiber recruitment functions with untreated vs. treated fiber orientation distributions were presented. Considering both the fiber orientation distributions and the fiber recruitment functions after GAG depletion did not improve prediction (rms = 0.141) as opposed to when using the untreated fiber orientation distributions (rms = 0.149).

The contribution to biaxial mechanics from each ECM constituent reveals that elastin is dominant over the range tested for both untreated and treated tissue (Fig. 8). The percent contribution from each ECM constituent at a physiologically relevant level of stretch (20%) is shown in Table 1. After treatment, medial collagen and to a lesser extent, adventitial collagen, contributes more to the mechanics, particularly in the circumferential direction. Compared to using the treated fiber distributions, when the untreated fiber distributions were used, the contribution from each ECM constituents to artery mechanics was slightly altered. The percent

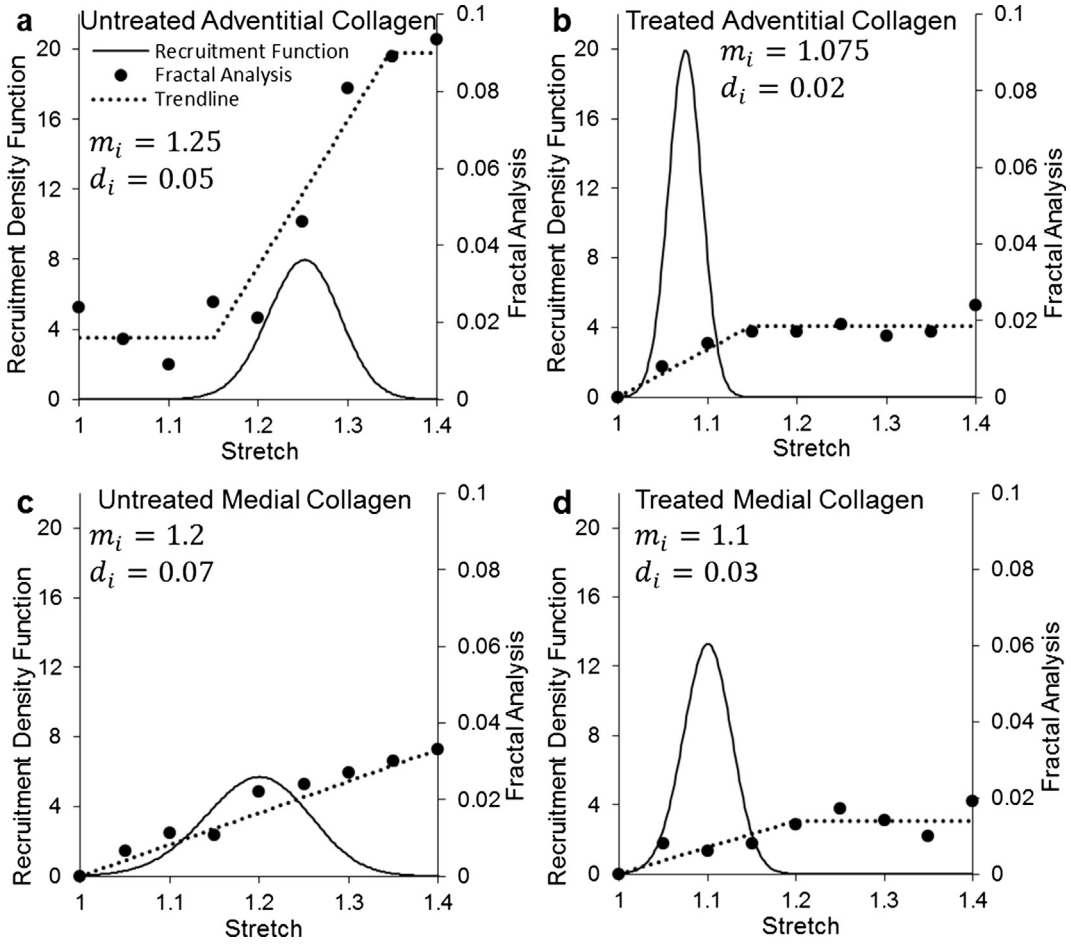

Fig. 5. Fractal analysis (circles and dashed line) and recruitment functions (solid curve) for adventitial collagen before (a) and after (b) GAG depletion, as well as medial collagen before (c) and after (d) GAG depletion. m_i and d_i are the mean and standard deviation of the fiber recruitment function. Untreated data from (Chow et al., 2014) and treated data from (Mattson et al., 2016) (n = 6). Error bars represent standard error of the mean.

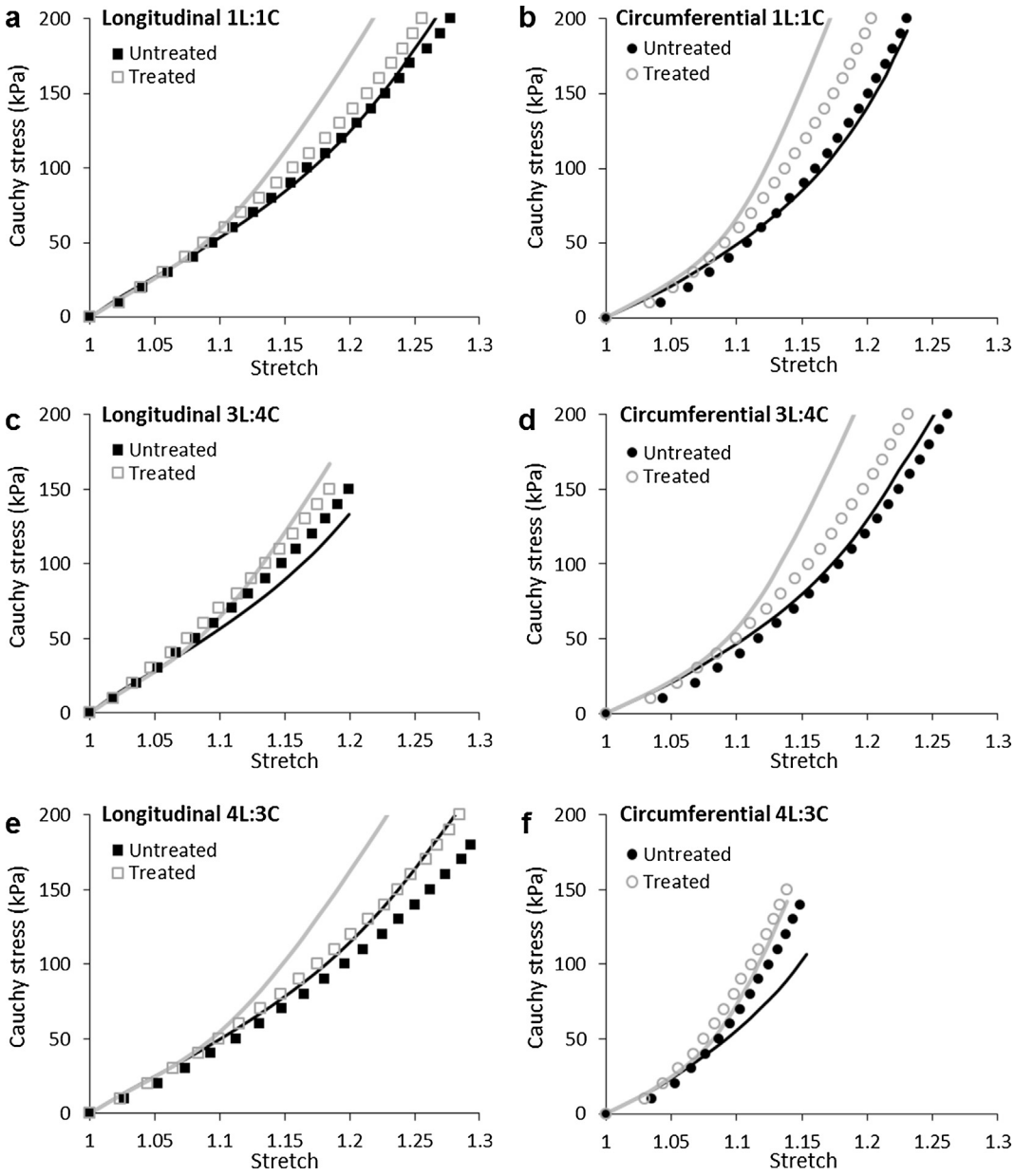

Fig. 6. Average stress-stretch experimental data (points) (n = 6) and model fit/prediction (lines) for untreated (black) and treated (gray) tissue in the longitudinal and circumferential directions with (a,b) 400:400 N/m, (c,d) 300:400 N/m, and (e,f) 400:300 N/m biaxial tension. Chain density ($n_{ME} = 3.01 \times 10^{25} 1/m^3$, $n_{MC} = 1.2510^{25} 1/m^3$, $n_{AC} = 1.2510^{24} 1/m^3$), rigid links per chain ($N_{ME} = 5, N_{MC} = 2.71, N_{AC} = 2.71$), root mean square error of fit (rmsf = 0.0135), and root mean square error of prediction (rmsp = 0.141).

contribution from longitudinal medial elastin decreased while the contribution of longitudinal medial and adventitial collagen increased. The opposite was true for the circumferential direction, where medial elastin contributed more, but medial and adventitial collagen contributed less.

4. Discussion

Using a structure-based constitutive model that incorporates changes in fiber recruitment due to GAG depletion, the present study successfully predicted the mechanical stiffening based on earlier fiber recruitment due to enzymatic GAG depletion. The collagen fiber distribution and recruitment functions are obtained directly from quantitative analysis of multiphoton microscopy images. Our study provides new understandings on the relationship among ECM constituents, elastin, collagen, and GAGs; and how they interact and contribute to vascular mechanics.

GAGs have been found to contribute to the mechanics of soft tissues such as cartilage, tendon, lung, eye sclera, and artery (Halper, 2014; Legerlotz et al., 2013; Mattson et al., 2016; Murienne et al., 2015; Sorrentino et al., 2015; Takahashi et al., 2014). In arteries, proteoglycans constitute only a minor component of vascular tissue (2%–5% by dry weight), however these macromolecules are of enormous importance in influencing arterial properties such as viscoelasticity, thrombosis, permeability, lipid metabolism, and hemostasis of the arterial wall (Berenson et al., 1984; Camejo, 1982; Mattson et al., 2016; Wight, 1989). Despite these earlier findings, potential mechanisms of GAGs contributing to tensile mechanics are not fully understood. Previous studies suggest GAGs either transmit loads between adjacent collagen fibrils by acting as a mechanical crosslink (Scott, 2003), or iso-

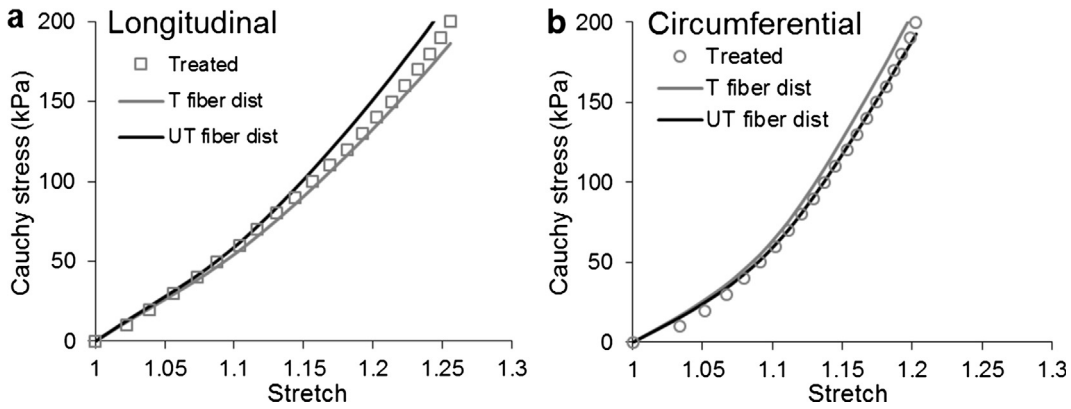

Fig. 7. Predicting the treated mechanics data (symbols) with treated fiber distributions (T fiber dist, rms = 0.149) does not improve the fit compared to using untreated fiber distributions (UT fiber dist, rms = 0.141) in the longitudinal (a) and circumferential (b) directions.

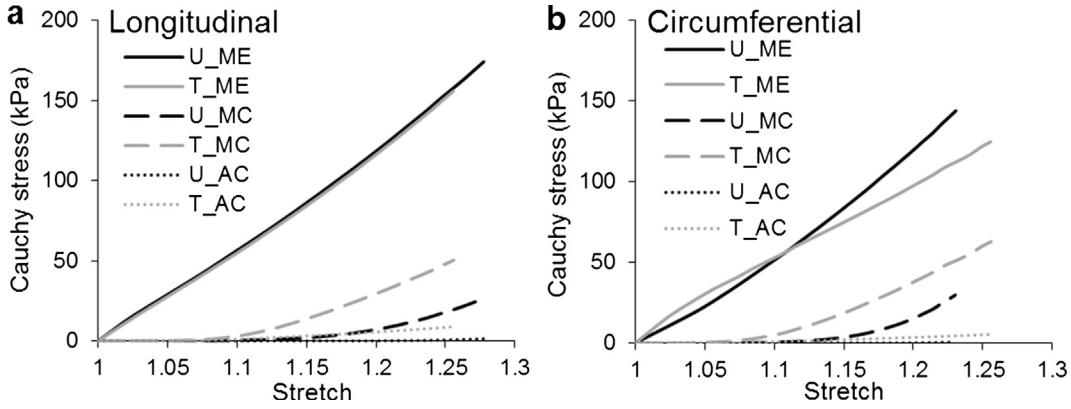

Fig. 8. Cauchy stress vs. stretch for medial elastin (ME, solid), medial collagen (MC, dashed), and adventitial collagen (AC, dotted) of untreated (U_, black) and treated (T_, gray) tissue in the longitudinal (a) and circumferential (b) directions.

Table 1
Percent contribution to mechanics at 1.2 stretch for medial elastin (ME), medial collagen (MC), and adventitial collagen (AC) of untreated and treated tissue in the longitudinal and circumferential directions. U/T uses untreated fiber distributions with treated fiber recruitment functions.

	Longitude			Circumference		
	ME	MC	AC	ME	MC	AC
Untreated	97.68	2.30	0.02	95.43	4.55	0.02
Treated	85.85	11.52	2.63	76.91	20.94	2.15
U/T	89.48	8.51	2.01	75.48	22.05	2.47

late adjacent fibers from shear friction and do not directly contribute to tensile stiffness (Rigozzi et al., 2013). Building upon the latter and according to the *slide-stuck* theory, a sufficient level of GAGs reduce fibril strain by allowing sliding rather than overstretch (Linka et al., 2016). Though the mechanism may be different, our findings are more consistent with the idea that GAGs protect collagen fibers from over-stretching since enzymatically depleting GAGs results in straighter fibers that are recruited at lower levels of stretch (Fig. 3). Furthermore, decreased elastin and GAG content from trypsin decellularization reduces fiber waviness (Lin et al., 2016), but since our enzyme treatment specifically targets GAGs, decreasing GAG content alone is sufficient for a loss of collagen fiber waviness (Fig. 1).

Fiber orientation distributions before and after enzymatic GAG depletion at 40% stretch were used (Fig. 2). For intact tissue, medial collagen is circumferentially oriented and becomes even more so after GAG removal. Medial elastin is relatively uniformly distributed with a slight longitudinal peak as well as a small circumferential peak emerging after GAG removal. Adventitial collagen has a preferred longitudinal orientation as well as a minor circumferential oreintation, but after GAG depletion, more distinct peaks emerge with a general shift towards the circumference. This is perhaps because GAGs are associated with collagen organization, so GAG depletion could lead to less organized fiber bundles with greater variation in orientation (Couchman and Pataki, 2012). Comparing the changes in fiber orientation distributions (Fig. 2) to changes in fiber contributions to each anatomical direction (Table 1) demonstrates that there is a close interplay between fiber recruitment and fiber orientation, and also among different fiber types. For example, the adventitial collagen fibers show more circumferential peaks in the treated fiber orientation distribution for (Fig. 2) and adventitial collagen contributed more to the circumferential direction in treated versus untreated tissue (Table 1). However, the fiber orientation distribution for medial elastin

showed minimal changes (Fig. 2), but the contribution of medial elastin decreased in the circumferential direction of treated tissue due to increased collagen recruitment (Table 1).

The fiber recruitment function in the present study was obtained directly based on fractal analysis of multiphoton microscopy images (Fig. 5). Fractal analysis serves as a broad measure of fiber recruitment for adventitial collagen as well as medial collagen and elastin, which has a finer, more intricate fiber network that cannot be traced with straightness parameter (Chow et al., 2014). In previous studies, collagen fiber recruitment was usually estimated in structure-based constitutive models (Cacho et al., 2007; Weisbecker et al., 2015; Zeinali-Davarani et al., 2015; Zulliger et al., 2004). Hill et al. (2012) measured medial collagen fiber tortuosity, the inverse of straightness parameter, based on multiphoton images of rabbit carotid artery. A gamma cumulative distribution function was then fit to the tortuosity data. However, uniaxial loading was used and the model assumes the rest of the arterial structure is an isotropic matrix (Hill et al., 2012). The present study employs biaxial loading, which is important to fully characterize the anisotropic mechanical behavior of aorta. The use of a straightness parameter of at least 0.98 to represent recruited fibers in Fig. 4 is consistent with the tortuosity of 1.02 by Hill et al. (2012). The left-skewed straightness parameter distributions in Fig. 3 complement and support fractal analysis (Fig. 5), since both show collagen fibers are being recruited at lower levels of stretch when GAGs are depleted.

Previous work on structure-based constitutive modeling of aorta considered GAGs to transfer load through "collagen-GAG complexes" (Polzer et al., 2015). Collagen fiber orientation was determined from histological analysis. In the present study, multiphoton microscopy was used to simultaneously image collagen and elastin in the aortic wall with minimum sample preparation. The model that incorporates changes in fiber recruitment due to GAG depletion provided a good fit to the untreated data as well as prediction of the treated biaxial data (Fig. 6). Our previous study has shown that the adventitial collagen fibers became significantly straighter and led to earlier stiffening with GAG removal (Mattson et al., 2016). Using the treated instead of untreated fiber orientation distributions only slightly affects the model's prediction of overall mechanics (rms = 0.141 vs 0.149, Fig. 7) as well as the relative contribution of each ECM constituent (Table 1).

An advantage of the constitutive model in this study is that the contribution of individual ECM constituents can be estimated (Fig. 8 and Table 1). At a physiological relevant stretch of 20%, elastin primarily contributes to the total stress, which is expected since collagen, particularly adventitial collagen, is to provide stiffening and prevent arterial rupture during exceptional cases of overextension (Hemmasizadeh et al., 2015; Wagenseil and Mecham, 2009). However, GAG depletion results in collagen being engaged at lower loading levels. As a result, the relative contribution of both medial and adventitial collagen to the total mechanical stress increases, and this change is more prominent in the circumferential direction. Such redistribution of stresses may hold significant implications in alterations of tissue homeostasis, which usually triggers a series of events in artery remodeling (Humphrey et al., 2014).

5. Limitations

Enzymatic GAG depletion is considered specific and effective, but we cannot entirely rule out an unobservable structural change. In the present model, the mechanical properties of elastin and collagen fibers and relative content are assumed to be the same before and after GAG depletion. Constraints were placed on the six free parameters of the constitutive model (n_i and N_i, i = ME, MC, and AC) to ensure a unique solution. However, this is reasonable since the constraints were relatively broad and based on physiologically realistic values. The changes in mechanical properties were attributed to changes in collagen fiber recruitment, which was obtained directly from multiphoton imaging analysis. The z-stack images were obtained from both the adventitial and intimal surfaces, but the middlemost portion of the arterial wall was not captured. Thus, the fiber orientation distributions may not reflect the full structure of arterial wall. Finally, fiber orientation and recruitment were measured in 2D instead of 3D, but a previous 3D study concluded that a planar assumption is justified since fibers were almost all less than 5° out of plane (Hill et al., 2012).

6. Conclusions

In this study, a structure-based constitutive model was adapted to successfully predict the changes to biaxial arterial mechanics due to the effect of GAGs on fiber recruitment. The model incorporates medial elastin, medial collagen, and adventitial collagen fiber distributions, recruitment, content, and fiber properties to determine tissue-level biomechanical function. Enzymatic GAG depletion shifts collagen fiber recruitment to lower levels of stretch with a corresponding earlier nonlinear stiffening. Additionally, successful fitting and predicting was accomplished with a small set of physically meaningful material parameters related to the structure and properties of the ECM constituents. Although GAGs constitute only a small faction component of vascular tissue, our studies suggest that in constitutive modeling their contribution to arterial mechanics should be considered through interactions with other ECM constituents, such as collagen. Results from this study may have clinical and physiological relevance to understanding mechanisms that affect vascular homeostasis and mechanobiology with associated alterations in GAG content such as aging, diabetes and atherosclerosis.

Conflict of interest statement

We declare that we have no financial or personal relationships with other people or organizations that could inappropriately influence (bias) our work.

Acknowledgement

This work was supported, in part, by a grant (CMMI 1463390) from National Science Foundation, and a pre-doctoral training grant (2T32HL007969) from National Institutes of Health.

References

Bartholomew, J.S., Anderson, J.C., 1983. Investigation of relationships between collagens, elastin and proteoglycans in bovine thoracic aorta by immunofluorescence techniques. Histochem. J. 15, 1177–1190.

Berenson, G.S., Radhakrishnamurthy, B., Srinivasan, S.R., Vijayagopal, P., Dalferes, E. R., Sharma, C., 1984. Recent advances in molecular pathology. Exp. Mol. Pathol. 41, 267–287. https://doi.org/10.1016/0014-4800(84)90043-1.

Boumaza, S., Arribas, S.M., Osborne-Pellegrin, M., McGrath, J.C., Laurent, S., Lacolley, P., Challande, P., 2001. Fenestrations of the carotid internal elastic lamina and structural adaptation in stroke-prone spontaneously hypertensive rats. Hypertens (Dallas, Tex. 1979) 37, 1101–1107.

Brüel, A., Oxlund, H., 1996. Changes in biomechanical properties, composition of collagen and elastin, and advanced glycation endproducts of the rat aorta in relation to age. Atherosclerosis 127, 155–165. https://doi.org/10.1016/S0021-9150(96)05947-3.

Cacho, F., Elbischger, P.J., Rodríguez, J.F., Doblaré, M., Holzapfel, G.A., 2007. A constitutive model for fibrous tissues considering collagen fiber crimp. Int. J. Non. Linear Mech., Special Issue in Honour of Dr Ronald S. Rivlin 42, 391–402. https://doi.org/10.1016/j.ijnonlinmec.2007.02.002.

Camejo, G., 1982. The interaction of lipids and lipoproteins with the intercellular matrix of arterial tissue: its possible role in atherogenesis. Adv. Lipid Res. 19, 1–53.

Campa, J.S., Greenhalgh, R.M., Powell, J.T., 1987. Elastin degradation in abdominal aortic aneurysms. Atherosclerosis 65, 13–21.

Chow, M.J., Choi, M., Yun, S.H., Zhang, Y., 2013a. The effect of static stretch on elastin degradation in arteries. PLoS ONE. 8,. https://doi.org/10.1371/journal.pone.0081951 e81951.

Chow, M.J., Mondonedo, J.R., Johnson, V.M., Zhang, Y., 2013b. Progressive structural and biomechanical changes in elastin degraded aorta. Biomech. Model. Mechanobiol. 12, 361–372. doi.org/10.1007/s10237-012-0404-9.

Chow, M.J., Turcotte, R.R., Lin, C.P.P., Zhang, Y., 2014. Arterial extracellular matrix: A mechanobiological study of the contributions and interactions of elastin and collagen. Biophys. J. 106, 2684–2692. https://doi.org/10.1016/j.bpj.2014.05.014.

Couchman, J.R., Pataki, C.A., 2012. An introduction to proteoglycans and their localization. J. Histochem. Cytochem. 60, 885–897. https://doi.org/10.1369/0022155412464638.

Eisenstein, R., Kuettner, K., 1976. The ground substance of the arterial wall Part 2. Electron-microscopic studies. Atherosclerosis 24, 37–46. https://doi.org/10.1016/0021-9150(76)90062-9.

Gandley, R.E., McLaughlin, M.K., Koob, T.J., Little, S.A., McGuffee, L.J., 1997. Contribution of chondroitin-dermatan sulfate-containing proteoglycans to the function of rat mesenteric arteries. Am. J. Physiol. 273, H952–H960.

Halper, J., 2014. Proteoglycans and diseases of soft tissues. In: Halper, J. (Ed.), Advances in Experimental Medicine and Biology, Advances in Experimental Medicine and Biology. Springer, Netherlands, pp. 49–58. https://doi.org/10.1007/978-94-007-7893-1_4.

Heegaard, A.-M.M., Corsi, A., Danielsen, C.C., Nielsen, K.L., Jorgensen, H.L., Riminucci, M., Young, M.F., Bianco, P., 2007. Biglycan deficiency causes spontaneous aortic dissection and rupture in mice. Circulation 115, 2731–2738. https://doi.org/10.1161/CIRCULATIONAHA.106.653980.

Hemmasizadeh, A., Tsamis, A., Cheheltani, R., Assari, S., D'Amore, A., Autieri, M., Kiani, M.F., Pleshko, N., Wagner, W.R., Watkins, S.C., Vorp, D., Darvish, K., 2015. Correlations between transmural mechanical and morphological properties in porcine thoracic descending aorta. J. Mech. Behav. Biomed. Mater. 47, 12–20. https://doi.org/10.1016/j.jmbbm.2015.03.004.

Hill, M.R., Duan, X., Gibson, G.A., Watkins, S., Robertson, A.M., 2012. A theoretical and non-destructive experimental approach for direct inclusion of measured collagen orientation and recruitment into mechanical models of the artery wall. J. Biomech. Special Issue Cardiovasc. Solid Mech. 45, 762–771. https://doi.org/10.1016/j.jbiomech.2011.11.016.

Holzapfel, G.A., Sommer, G., Gasser, C.T., Regitnig, P., Gerhard, A., 2005. Determination of layer-specific mechanical properties of human coronary arteries with nonatherosclerotic intimal thickening and related constitutive modeling. Am. J. Physiol. Heart Circ. Physiol. 289 (5), H2048–H2058. https://doi.org/10.1152/ajpheart.00934.2004.

Huang, F., Thompson, J.C., Wilson, P.G., Aung, H.H., Rutledge, J.C., Tannock, L.R., 2008. Angiotensin II increases vascular proteoglycan content preceding and contributing to atherosclerosis development. J. Lipid Res. 49, 521–530. https://doi.org/10.1194/jlr.M700329-JLR200.

Humphrey, J.D., 2012. Possible mechanical roles of glycosaminoglycans in thoracic aortic dissection and associations with dysregulated transforming growth factor-β. J. Vasc. Res. https://doi.org/10.1159/000342436.

Humphrey, J.D., Dufresne, E.R., Schwartz, M.A., 2014. Mechanotransduction and extracellular matrix homeostasis. Nat. Rev. Mol. Cell Biol. 15, 802–812. https://doi.org/10.1038/nrm3896.

Humphrey, J.D., Holzapfel, G.A., 2012. Mechanics, mechanobiology, and modeling of human abdominal aorta and aneurysms. J. Biomech. 45, 805–814. https://doi.org/10.1016/j.jbiomech.2011.11.021.

Jensen, T., 1997. Pathogenesis of diabetic vascular disease: evidence for the role of reduced heparan sulfate proteoglycan. Diabetes 46 (Suppl 2), S98–S100. https://doi.org/10.2337/diab.46.2.S98.

Lai, W.M., Hou, J.S., Mow, V.C., 1991. A triphasic theory for the swelling and deformation behaviors of articular cartilage. J. Biomech. Eng. 113, 245–258. https://doi.org/10.1115/1.2894880.

Lanir, Y., 1979. A structural theory for the homogeneous biaxial stress-strain relationships in flat collagenous tissues. J. Biomech. 12, 423–436. https://doi.org/10.1016/0021-9290(79)90027-7.

Lee, R.T., Yamamoto, C., Feng, Y., Potter-Perigo, S., Briggs, W.H., Landschulz, K.T., Turi, T.G., Thompson, J.F., Libby, P., Wight, T.N., 2001. Mechanical strain induces specific changes in the synthesis and organization of proteoglycans by vascular smooth muscle cells. J. Biol. Chem. 276, 13847–13851. https://doi.org/10.1074/jbc.M010556200.

Legerlotz, K., Riley, G.P., Screen, H.R.C., 2013. GAG depletion increases the stress-relaxation response of tendon fascicles, but does not influence recovery. Acta Biomater. 9, 6860–6866. https://doi.org/10.1016/j.actbio.2013.02.028.

Lewis, P.N., Pinali, C., Young, R.D., Meek, K.M., Quantock, A.J., Knupp, C., 2010. Structural interactions between collagen and proteoglycans are elucidated by three-dimensional electron tomography of Bovine Cornea. Structure 18, 239–245. https://doi.org/10.1016/j.str.2009.11.013.

Li, J., Du, Q., Sun, C., 2009. An improved box-counting method for image fractal dimension estimation. Lect. Notes. Comput. Sci. 42, 2460–2469. https://doi.org/10.1016/j.patcog.2009.03.001.

Lin, C.H., Kao, Y.C., Lin, Y.H., Ma, H., Tsay, R.Y., 2016. A fiber-progressive-engagement model to evaluate the composition, microstructure, and nonlinear pseudoelastic behavior of porcine arteries and decellularized derivatives. Acta Biomater. 46, 101–111. https://doi.org/10.1016/j.actbio.2016.09.025.

Linka, K., Khiêm, V.N., Itskov, M., 2016. Multi-scale modeling of soft fibrous tissues based on proteoglycan mechanics. J. Biomech. Cardiovasc. Biomech. Health Dis. 49, 2349–2357. https://doi.org/10.1016/j.jbiomech.2016.02.049.

Little, P.J., Ballinger, M.L., Osman, N., 2007. Vascular wall proteoglycan synthesis and structure as a target for the prevention of atherosclerosis. Vasc. Health Risk Manage.

Martinez-Lemus, L.A., Hill, M.A., Meininger, G.A., 2009. The plastic nature of the vascular wall: a continuum of remodeling events contributing to control of arteriolar diameter and structure. Physiol. (Bethesda) 24, 45–57. https://doi.org/10.1152/physiol.00029.2008.

Mattson, J.M., Turcotte, R., Zhang, Y., 2016. Glycosaminoglycans contribute to extracellular matrix fiber recruitment and arterial wall mechanics. Biomech. Model. Mechanobiol. 16, 1–13. https://doi.org/10.1007/s10237-016-0811-4.

Menashi, S., Campa, J.S., Greenhalgh, R.M., Powell, J.T., 1987. Collagen in abdominal aortic aneurysm: typing, content, and degradation. J. Vasc. Surg. 6, 578–582.

Mow, V.C., Kuei, S.C., Lai, W.M., Armstrong, C.G., 1980. Biphasic creep and stress relaxation of articular cartilage in compression: theory and experiments. J. Biomech. Eng. 102, 73–84. https://doi.org/10.1115/1.3138202.

Murienne, B.J., Jefferys, J.L., Quigley, H.A., Nguyen, T.D., 2015. The effects of glycosaminoglycan degradation on the mechanical behavior of the posterior porcine sclera. Acta Biomater. 12, 195–206. https://doi.org/10.1016/j.actbio.2014.10.033.

Polzer, S., Gasser, T.C., Novak, K., Man, V., Tichy, M., Skacel, P., Bursa, J., 2015. Structure-based constitutive model can accurately predict planar biaxial properties of aortic wall tissue. Acta Biomater. 14, 133–145. https://doi.org/10.1016/j.actbio.2014.11.043.

Rigozzi, S., Müller, R., Stemmer, A., Snedeker, J.G., 2013. Tendon glycosaminoglycan proteoglycan sidechains promote collagen fibril sliding-AFM observations at the nanoscale. J. Biomech. 46, 813–818. https://doi.org/10.1016/j.jbiomech.2012.11.017.

Schaefer, L., Schaefer, R.M., 2010. Proteoglycans: from structural compounds to signaling molecules. Cell Tissue Res. 339, 237–246. https://doi.org/10.1007/s00441-009-0821-y.

Scott, J.E., 2003. Elasticity in extracellular matrix "shape modules" of tendon, cartilage, etc. A sliding proteoglycan-filament model. J. Physiol. 553, 335–343. https://doi.org/10.1113/jphysiol.2003.050179.

Sorrentino, T.A., Fourman, L., Ferruzzi, J., Miller, K.S., Humphrey, J.D., Roccabianca, S., 2015. Local versus global mechanical effects of intramural swelling in carotid arteries 041008 041008 J. Biomech. Eng. 137. https://doi.org/10.1115/1.4029303.

Takahashi, A., Majumdar, A., Parameswaran, H., Bartolák-Suki, E., Suki, B., 2014. Proteoglycans maintain lung stability in an elastase-treated mouse model of emphysema. Am. J. Respir. Cell Mol. Biol. 51, 26–33. https://doi.org/10.1165/rcmb.2013-0179OC.

Vorp, D.A., 2007. Biomechanics of abdominal aortic aneurysm. J. Biomech. 40, 1887–1902. https://doi.org/10.1016/j.jbiomech.2006.09.003.

Wagenseil, J.E., Mecham, R.P., 2009. Vascular extracellular matrix and arterial mechanics. Physiol. Rev. 89, 957–989. https://doi.org/10.1152/physrev.00041.2008.

Wang, Y., Zeinali-Davarani, S., Zhang, Y., 2016. Arterial mechanics considering the structural and mechanical contributions of ECM constituents. J. Biomech. 49, 2358–2365. https://doi.org/10.1016/j.jbiomech.2016.02.027.

Weisbecker, H., Unterberger, M.J., Holzapfel, G.A., 2015. Constitutive modelling of arteries considering fibre recruitment and three-dimensional fibre distribution. J. Roy. Soc. Interface 12, 20150111-. https://doi.org/10.1098/rsif.2015.0111.

Wight, T.N., 1989. Cell biology of arterial proteoglycans. Arteriosclerosis 9, 1–20. https://doi.org/10.1161/01.ATV.9.1.1.

Wight, T.N., Merrilees, M.J., 2004. Proteoglycans in atherosclerosis and restenosis: key roles for versican. Circ. Res. 94, 1158–1167. https://doi.org/10.1161/01.RES.0000126921.29919.51.

Zeinali-Davarani, S., Wang, Y., Chow, M.-J., Turcotte, R., Zhang, Y., 2015. Contribution of collagen fiber undulation to regional biomechanical properties along porcine thoracic aorta. J. Biomech. Eng. 137, 51001. https://doi.org/10.1115/1.4029637.

Zhang, Y., Dunn, M.L., Drexler, E.S., et al., 2005. A microstructural hyperelastic model of pulmonary arteries under normo- and hypertensive conditions. Ann. Biomed. Eng. 33, 1042–1052. https://doi.org/10.1007/s10439-005-5771-2.

Zulliger, M.A., Fridez, P., Hayashi, K., Stergiopulos, N., 2004. A strain energy function for arteries accounting for wall composition and structure. J. Biomech. 37, 989–1000. https://doi.org/10.1016/j.jbiomech.2003.11.026.